Biomimetic ion substituted hydroxyapatite coating on surgical grade 316L SS for implant applications

K. Prem Ananth[1*], Sujin P. Jose[2,4], A. Joseph Nathanael[3], Tae Hwan Oh[3], D. Mangalaraj[1], A. M. Ballamurugan[1*]

[1]*Department of Nanoscience and Technology, Bharathiar University, Coimbatore 641046, India*
[2]*Department of Materials Science and Nano Engineering, Rice University, Texas 77005, USA*
[3]*Department of Nano, Medical and Polymer Materials, Yeungnam University, Gyeongsan 712749, South Korea*
[4]*School of Physics, Madurai Kamaraj University, Madurai 625021, India*

[*]Corresponding author. Tel: (+91) 422-2425458; E-mail: kpananth01@gmail.com (K.P. Ananth);
Tel.: (+91) 422-2428421; E-mail: balamurugan@buc.edu.in (A.M. Ballamurugan)

ABSTRACT

In this paper, we have reported a successful synthesis of ionic substituted (Si, Sr and Zn) hydroxyapatite (HAp) using chemical precipitation method and the coating of the synthesized materials on surgical grade 316 L SS using electrophoretic deposition technique. The structural, compositional, functional group and morphological characterization of the developed coatings were carried out using XRD, EDX, FT-IR, and FE-SEM. Electrochemical studies such as potentiodynamic polarization, electrochemical impedance studies were performed to evaluate the corrosion resistance imparted by the coatings and was found that considerable resistance was exhibited by the coated samples. Furthermore the coated samples were tested for in-vitro biomineralization ability in simulate body fluid (SBF) solution at different immersion time periods and was found that the thickness of the apatite film was increased with the increase in the immersion time and the surface became entirely covered with apatite. Thus it is opined that the developed Si, Sr, and Zn substituted Hydroxyapatite (I-HAp) coating on 316 L SS substrate would be ideal candidates for bio implant applications. Copyright © 2015 VBRI Press.

Keywords: Hydroxyapatite; 316 L SS; corrosion protection; ion substitution.

Introduction

Inorganic bioceramic hydroxyapatite (HAp), being the main inorganic composition of the hard tissues in natural bones, has been extensively studied for medical application due to its excellent bioactivity and biocompatibility [1]. Natural bone composed of calcium phosphate mineral, which is in apatite phase with trace elements such as bivalent cation Zn^{2+}, Ca^{2+}, Sr^{2+}, Ba^{2+}, Mg^{2+}, Cd^{2+}, and Pb^{2+}. Monovalent cation/anion Na^+, K^+, OH^-, F^-, Cl^-, and Br- and trivalent cation/anion Al^{3+}, PO_4^{3-}, VO_4^{3} and SO_4^{3-} embedded in it play very crucial role in the biological and mechanical performance of the bone [2]. The HAp coating on metallic implants alone is not sufficient due to their low wear resistance. They tend to get dissoluted from the surface of metal before it could impart its role in bone formation and also it is less bioactive, thus the ossification and mineralization rate will be slower. In order to improve its bone remodeling ability such as increase in mechanical strength, improved biological properties and enzymatic activity. The increased ossification rate and controlled dissolution rate are thereby fastening the repair mechanism and making it highly suitable for implant applications [3-

10]. Silica an essential trace element, has role in osteoblast proliferation, differentiation, collagen production, cell matrix attachment, decreasing the resorption rate and increasing the alkaline phosphates activity which is an indicator of bone remodeling process [11, 12]. Strontium (ionic radius 0.12 nm) that substitutes for Ca (ionic radius 0.0999 nm) in the HAp structure has antiresorptive property and has role in osteoblast differentiation [13, 14]. Zinc ion incorporation has been demonstrated to have stimulatory effects bone mineralization and also has role in stimulating the gene expression for proteins such as osteopontin and osteonectin [15-18]. Metallic implant materials suh as 316 L stainless steel, cobalt- chromium-alloys and titanium alloys are widely used for dental and orthopaedic implant applications. Among these metals, austenitic 316 L SS possesses reasonable biocompatibility, tensile strength and fatigue resistance [19]. Various methods have been adopted to coat the apatite on the metallic substrates, such as plasma spraying, chemical vapour deposition and pulsed laser, all of which work under high temperatures. These are complicated and time consuming techniques. But electrophoretic deposition method is relatively an easy method which works under low

temperature and it is possible to obtain a uniform crystalline deposit with low residual stresses [**20**]. It has also been reported that it is possible to control the coating thickness and morphology by manipulating the deposition voltage and time and it is considered to be one of the most promising method to obtain homogenous coating on metals [**21**].

The present paper deals with the incorporation of Si, Sr, and Zn ions into the HAp structure and coating on the 316 L SS substrate using electrophoretic deposition. To the best of our knowledge, so far very limited reports are available on the incorporation of three-ions (Si, Sr, Zn) into the HAp structure and coating on 316 L SS substrate. Hence the present work is designed to achieve the I-HAp coating on 316 L SS for improving the biomineralization ability and corrosion protection properties of the coatings. Thus the obtained I-HAp coated on 316 L SS substrate will serve as a potential candidate for biomedical implant application.

Experimental

Materials

Commercially available calcium nitrate tetra hydrate $((Ca(NO_3)_2.4H_2O)$, diammonium hydrogen phosphate $((NH_4)_2HPO_4)$, ammonium hydroxide (NH_4OH), tetraethyl orthosilicate (TEOS, $Si(OCH_2CH_3)_4$), strontium nitrate $Sr(NO3)2$, and zinc nitrate tetrahydrate $Zn(NO_3)_2.6H_2O$ were purchased from Sigma Aldrich Chemical and Co. (Aldrich, India). All the chemicals used were of analytical grade, and deionized water was used thought the experiment.
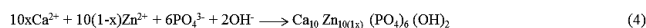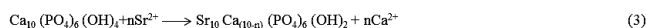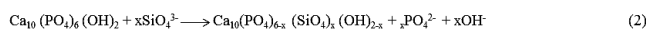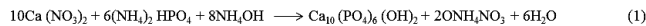
Material synthesis

For HAp and I-HAp were prepared by chemical precipitation method as showed in **Fig. S1**. The calcium nitrate tetrahydrate $(Ca(NO_3)_2.4H_2O)$, and diammonium hydrogen phosphate $(NH_4)_2 HPO_4$ were taken as calcium and phosphate precursors, respectively. For silica, strontium and zinc ion incorporation, tetraethylorthosilicate (TEOS, $Si(OCH_2CH_3)_4$), strontium nitrate $Sr(NO_3)_2$ and zinc nitrate tetrahydrate $Zn(NO_3)_2.6H_2O$ were taken respectively. The molar concentrations of the precursors were taken in such a way that the molar ratio of Ca and phosphate along with the substituted ions were equal to 1.67 for all compositions and the details of which are given in **Table 1**.

Table 1. Molar ratio of HAp, Si-HAp, Sr-HAp, Zn-HAp and I-Hap.

Sample	Ca(NO₃)₂.4H₂O (mole)	(NH₄)₂HPO₄ (mole)	Si(OCH₂CH₃)₄ (mole)	Sr(NO₃)₂ (mole)	(Zn(NO₃)₂.6H₂O) (mole)	Ca/P Molar Ratio	Ca+Sr+Zn/P+Si Molar ratio	Wt. in 100 mL Ca	P	Si	Sr	Zn
HAp	1.50	0.898	-	-	-	1.67	1.67	35.41	11.8	-	-	-
Si-HAp	1.50	0.862	0.0375	-	-	1.74	1.67	35.41	11.3	0.78	-	-
Sr-HAp	1.45	0.898	-	0.05	-	1.62	1.67	34.25	11.8	-	1.05	-
Zn-HAp	1.47	0.898	-	0.03	-	1.63	1.67	34.70	11.8	-	-	0.89
Si, Sr, Zn,HAp	1.45	0.862	0.0375	0.05	0.033	1.60	1.72	34.25	11.3	0.78	1.05	0.89

The precursors for ions were added while calcium nitrate tetrahydrate aqueous solution was under stirring, followed by drop wise addition of the diammonium hydrogen phosphate solution. The final solution was allowed for stirring at 750 rpm for 2 h. The pH of the

solution was maintained as 9 by adding proper amount of ammonium hydroxide (NH_4OH) solution. Then the suspension was kept at room temperature to allow the particles to settle down, which was washed with distilled water, centrifuged and dried in hot air oven at 120 ℃ for 24 h. The obtained powder was sintered at 900 ℃ for 2 h. The formation of Hap, Si-HAp, Sr-HAp, Zn-Hap and Si-Sr-Zn-HAp were described by the following equations

$$10Ca(NO_3)_2 + 6(NH_4)_2HPO_4 + 8NH_4OH \longrightarrow Ca_{10}(PO_4)_6(OH)_2 + 2ONH_4NO_3 + 6H_2O \qquad (1)$$

$$Ca_{10}(PO_4)_6(OH)_2 + xSiO_4^{3-} \longrightarrow Ca_{10}(PO_4)_{6-x}(SiO_4)_x(OH)_{2-x} + _xPO_4^{2-} + xOH^- \qquad (2)$$

$$Ca_{10}(PO_4)_6(OH)_4 + nSr^{2+} \longrightarrow Sr_{10}Ca_{(10-n)}(PO_4)_6(OH)_2 + nCa^{2+} \qquad (3)$$

$$10xCa^{2+} + 10(1-x)Zn^{2+} + 6PO_4^{3-} + 2OH^- \longrightarrow Ca_{10}Zn_{10(1x)}(PO_4)_6(OH)_2 \qquad (4)$$

Electrophoretic deposition HAp, Si-HAp, Sr-HAp, Zn-HAp and I-HAp

The 316 L stainless steel electrodes of 10 mm x 10 mm x 2 mm size were mechanically polished by silica carbide papers with grit sizes of 80 to 1000 followed by polishing using 1µm diamond paste to get a mirror like finish. The electrodes were washed thoroughly with running distilled water, rinsed and ultrasonically degreased with acetone and dried. The electrophoretic deposition process was carried out at room temperature from 2.5 g of pure I- HAp suspension in 80 ml isopropanol. The suspensions were stirred using Teflon paddle at 750 rpm in a magnetic stirrer. A platinum sheet of 30 mm x 90 mm x 1 mm dimension was used as the anode and the working electrode was used as the cathode. The distance between the anode and cathode was maintained to be 1 cm. The deposition was performed on 1 cm^2 surface area on one side of the specimen. The outer side and edge are masked with non-conducting Teflon tape. The voltage applied was between 90 and 150 V for a constant time period of 3 min. The coated samples were heat treated at 400 ℃. This same procedure was adopted for HAp, Si-HAp, Sr-HAp, and Zn-HAp coatings on 316 L SS.

Preparation of simulated body fluid (SBF)

The concentrations of different ions taken for the preparation of SBF solution are listed in the **Table S2**. It was prepared by dissolving appropriate quantities of reagent grade NaCl, NaHCO$_3$, KCl, Na$_2$HPO$_4$.2H$_2$O, MgCl$_2$.6H$_2$O, CaCl$_2$.2H$_2$O, Na$_2$SO$_4$ and Tris buffer into double distilled water. 1M HCl was used to maintain the pH at 7.4 at 37 °C. All the chemicals used in this study were of analytical grade obtained from Sigma Aldrich. The samples were immersed in SBF solution for different time intervals and gently rinsed with pure water and dried at room temperature and used further for SEM analysis.

Electrochemical corrosion analysis

Cyclic polarization experiments and electrochemical impedance analysis were carried out for evaluation of corrosion behavior of HAp, Si-HAp, Sr-HAp, Zn-HAp and I- HAp coatings on 316 L SS. The localized corrosion behaviors of the samples were studied in simulated body fluid (SBF) solution. The electrochemical cell of 500 mL capacity fitted with saturated calomel electrode (SCE) as a reference electrode, platinum foil as an auxiliary electrode

and coated 316 L SS as a working electrode was used for all measurements. The working electrode has a test surface area of 1 cm^2. The pH of the electrode was adjusted to 7.4 and temperature was maintained at 37 °C. All the electrochemical tests were carried out using potentiostat galvanostat (PGZ 301, Dynamic EIS, Tacussel, and Radiometer Copenhagen) with the electrochemical interface controlled by commercial software. The polarization study was carried out by increasing the potential at the scan rate of 1 mV/s. In order to obtain the average value, all the experiments were triplicated in SBF solution. The impedance spectra were acquired in the frequency range 10-5-10-1 Hz with a 10 mV amplitude sine wave generated by a frequency response analyzer.

Characterization techniques

To determine the phase purity of the synthesized material, X-ray diffraction (XRD) was performed (Bruker D8 Advance) with Cu-Kα radiation, 40 kV/40 mA, λ = 1.5406 nm. The data were collected between 25º and 40º 2θ using a step size of 0.02º with a count time of 2.5 seconds at each step. Phase identification was carried out by comparing the peak positions of the diffraction patterns with ICDD (JCPDS) standards. The functional groups were characterized by FTIR technique using Nicolet 8600 FTIR spectrometer. FTIR spectra were recorded from 400 to 4000 cm^{-1} with 4 cm^{-1} resolution averaging 100 scans. 2 mg of each sample was mixed with 300 mg of KBr and was pressed into a disk for the measurement. The surface morphologies of the HAp before and after coating were examined by field emission scanning electron microscopy (FESEM, Quanta 250 FEG, FEI Company) at 3 kV. The compositions of the samples were examined by EDXA (X Flash Detector, 5030 Bruker Nano, Germany).

Results and discussion

Morphological analysis of the coated and uncoated HAp, Si-HAp, Sr-HAp, Zn-HAp and I-HAp

Fig. 1 shows the FE-SEM images for the pure HAp, Si-HAp, Sr-HAp, Zn-HAp and I- HAp sintered at 900 ºC for 2 h. The image for the pure HAp in **Fig. 1(a)** shows the 3D prism like morphology with the size of 60 nm. The morphologies of the different ions substituted samples in **Fig. 1(b-e)** show the sphere like particle formation of homogeneous and interconnected network. The small particles got agglomerated with microspores formed within the interconnected network. However, no significant morphology difference was observed by incorporation of ions on HAp. The morphology of the HAp, Si-HAp, Sr-HAp, Z-HAp and I-HAp coated on 316 L SS are shown in **Fig. 2**. Dispersed particles with square shape are observed for HAp in **Fig. 2(a)**. The ion incorporated HAp has dumbbell shaped porous structure, which are closely packed together. Almost uniform microstructures are observed for all the coated samples seen in **Fig. 2(b-e)**. The cross sectional view of the coatings is around 18- 20 µm for both pure HAp and I- HAp. No major difference is observed for the coated HAp and I-HAp. **Fig. 2 (f, g, h, I, j)** shows the quantitative EDX analysis of HAp, Si-HAp, Sr-HAp, Zn-HAp and I-HAP respectively, which confirms

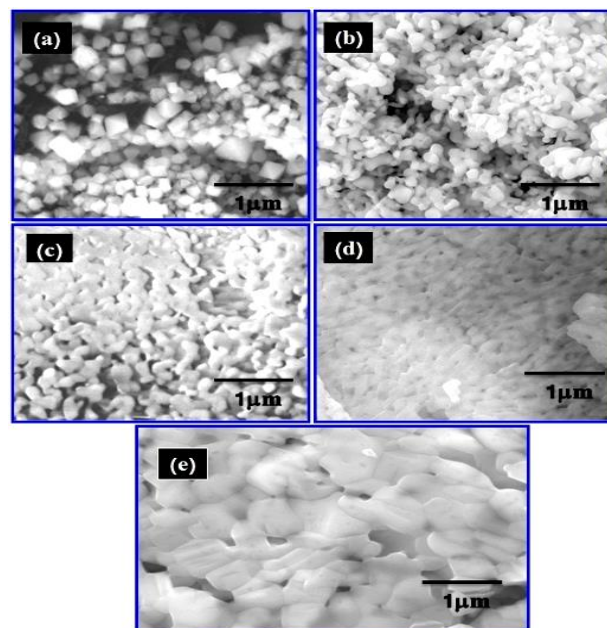the presence of all the species introduced during the synthesis step.

Fig. 1. FE-SEM images of (a) HAp, (b) Si-HAp, (c) Sr-HAp, (d) Zn-HAp and (e) I-HAp powdered samples.
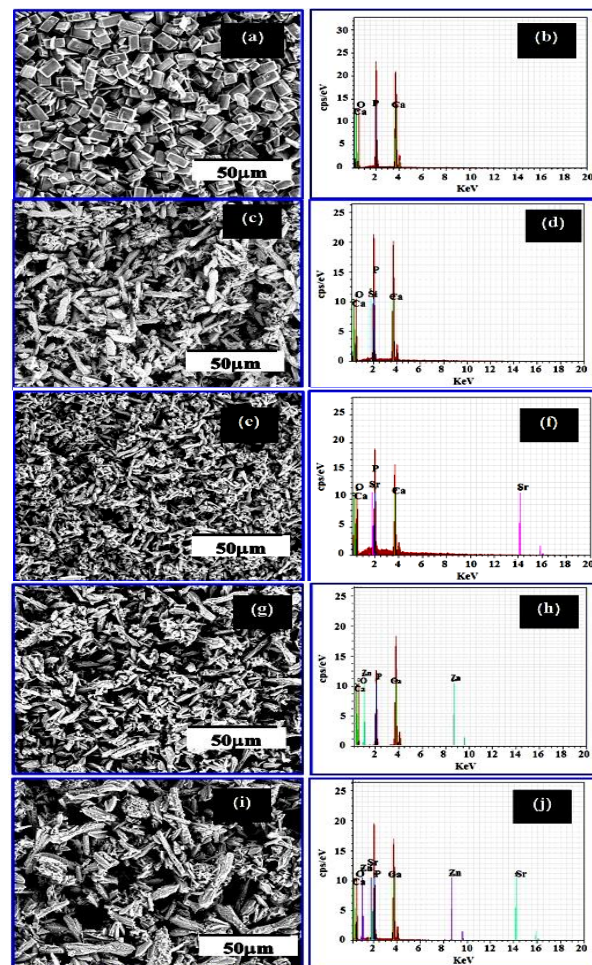

Fig. 2(a-j). FESEM Images and EDX analysis of (a, b) HAp, (c, d) Si-HAp, (e, f) Sr-HAp, (g, h) Zn-HAp and (I, j) I-HAp coated on 316 L SS.

It shows the successful incorporation of ions such as Si, Sr, and Zn in HAp. Also the weight percentages of various species taken while synthesis (**Table. 1**) is nearly equal to the weight percentages obtained in EDX analysis (**Table. S3**). No other peaks are obtained that confirms the purity of the samples.

Structural analysis of coated and uncoated HAp, Si-HAp, Sr-HAp, Zn-HAp and I-HAp

Fig. 3(a) shows the XRD pattern for the HAp, Si-HAp, Sr-HAp, Zn-HAp and I-HAp prepared by chemical precipitation method sintered at 900 °C for 2 h. The majority of the diffraction peaks match very well with the HAp phase. The 2θ values of 25.50, 31.41, 33.20, 39.43, 46.82 and 49.68 obtained correspond to HAp (002), (211), (222), (212), (222) and (213) reflection planes respectively and it is in good accord with the standard JCPDS card # 09-0438. Substitution of individual Si, Sr, and Zn ions, and incorporation of all these three ions in HAp structure cause no major change in the diffraction pattern except a little decrease in the intensity. No additional peaks are observed in the XRD pattern for the ions substituted HAp. The average crystallite size of the samples is estimated using the Scherer formula. The estimated average grain size for the pure HAp is 47 nm and it is found that with the individual incorporation of Si, Sr and Zn ions, the crystallite size is decreased to 46.25, 45.75 and 45.5 nm respectively. It is further decreased to 44.87 when all the three ions are incorporated.
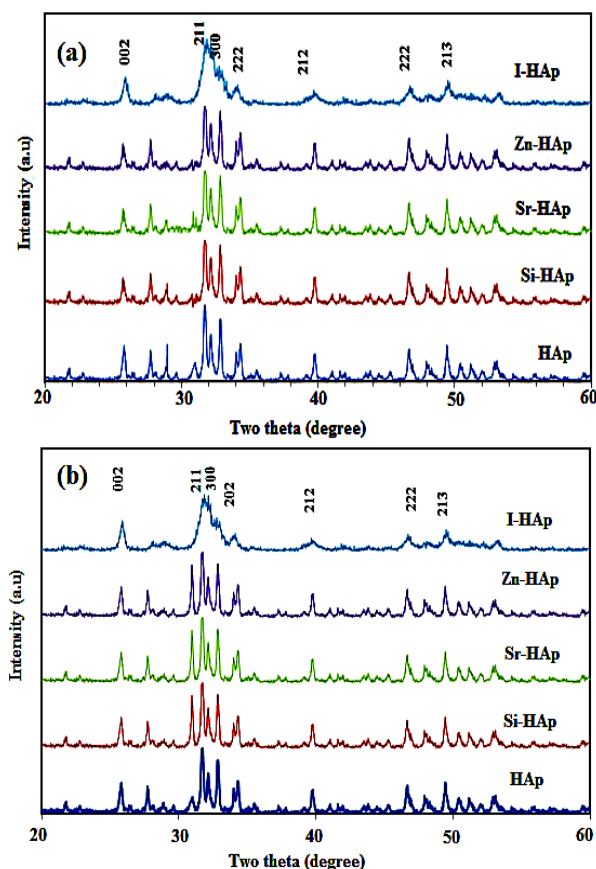
Fig. 3(b) shows the XRD pattern of the pure HAp and ion substituted HAp coatings on 316 L SS that was heat-treated at 400 °C for 2 h. There is no significant difference in the XRD pattern for the coated and uncoated samples in the pure HAp as well as in the I- HAp. While all coatings show the existence of Hap, ions incorporated HAp shows a small broadening of the peak and reduction in the intensity. All the I- HAp coatings on 316 L SS retain the hexagonal structure which is again in good agreement with the standard JCPDS Card # 09-0438. The crystallite size of the pure HAp coated on stainless steel is estimated as 71 nm. The crystallite size decreases to 70.5, 69 and 67.63 on the incorporation of Si, Sr and Zn respectively. It further decreases to 66 nm when all the three ions are incorporated. It may be presumably due to increase in amorphous nature with the incorporation of the ions.

Functional group analysis of HAp, Si-HAp, Sr-HAp, Zn-HAp and I-HAp

Fig. 4 shows the FT-IR spectra of HAp Si-HAp, Sr-HAp, Zn-HAp and I-HAp sintered at 900 °C. The peaks for PO_4^{3-} at 972, 565, 604, and 1091 cm^{-1} correspond to v_2 bending, v_4 bending, and v_1 stretching and v_3 asymmetric stretching vibration modes respectively. The peak at 3567 cm^{-1} indicates the presence of stretching modes of the hydroxyl (OH^-) group. Also the sharp peak at 635 cm^{-1} can be attributed to the bending vibration of hydroxyl group. The peaks at 875-962 and 1457 cm^{-1} can be attributed to CO_3^{2-} which arises from the atmospheric air during subsequent sample handling steps. The peaks corresponding to the stretching and bending modes of vibration of phosphate remain unaffected by the ionic substitution in HAp. All these obtained peaks confirm the formation of HAp.
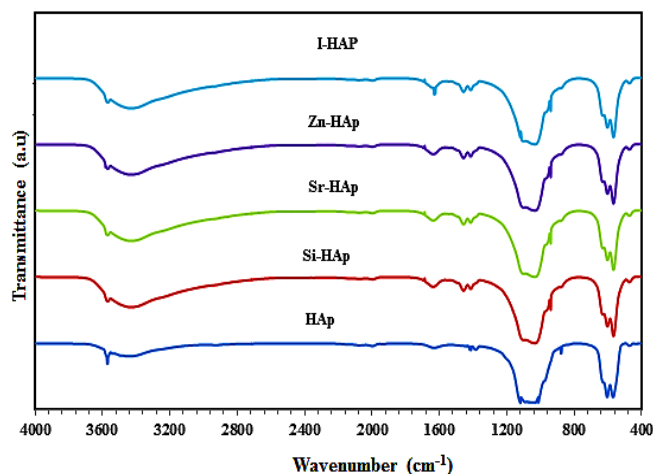

Fig. 3. XRD pattern of (a) Uncoated and (b) Coated HAp, Si-HAp, Sr-HAp, Zn-HAp and I-Hap.

Fig. 4. FT-IR Spectra of HAp, Si-HAp, Sr-HAp, Zn-HAp and I-HAp sintered at 900 °C.

In vitro biomineralization assessment in simulated body fluid (SBF) solution

The simulated body fluid (SBF) analysis was carried out to find the biomineralization ability of the I-HAp coated 316 L SS to form the apatite layer. **Fig. 5** shows the FE-SEM

images of I-HAp coated on 316 L SS, immersed in SBF for the duration of 7, 14 and 21 days. It is observed that on 7th day small granules of apatite start to form and subsequently formation of dense layer on 14th and 21st days. The whole surface of the sample is completely covered, which confirms the effect of biomineralization ability of the present coated substrate.
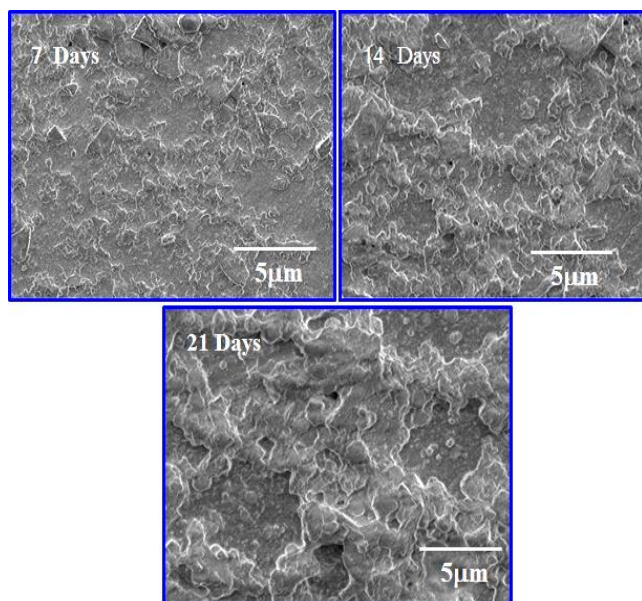

Fig. 5. FE-SEM images of I-HAp on 7th, 14th and 21st days of incubation in SBF.

In Vitro electrochemical analysis

Cyclic polarization: The cyclic polarization curves of bare, HAp, Si-HAp, Sr-HAp, Zn-HAp and I-HAp coated 316 L SS samples are shown in **Fig. 6(a)**. The corrosion potential (Ecorr) and the corrosion current density (Icorr) values for the bare 316 L SS are found to be -821 and 1.12 $\mu A/cm^2$ respectively. **Table 2** shows the corrosion kinetics parameters for HAp and various I-HAp coatings on 316 L SS. Corrosion potentials (Ecorr) for all the coated samples are higher than for the bare samples. I-HAp coated 316 L SS samples show a shift in positive direction when compared to the bare 316 L SS. Thus the corrosion potentials for all the coated samples are nobler than for the bare 316 L SS. Thus it is evident from the results that the coated samples demonstrate improved corrosion resistance than the uncoated samples.

Impedance analysis: **Fig. 6(b)** shows the impedance spectra for bare, HAp, Si-HAp, Sr-HAp, Zn-HAp and I-HAp coated on 316 L SS in simulated body fluid solution. All the coated samples show a typical spectrum of passivated surface similar to capacitive behavior. The Rb values show significant increase for ionic substituted HAp than bare HAp. **Table. 2** lists the high capacitance values observed for bare 316 L SS. The capacitance (C) obtained at the respective breakdown potentials are found to decrease in HAp from the corresponding values for ion substituted HAp coated samples. The electrochemical impedance spectra analysis shows agreement of all values with the reported data. This result confirms that the

materials are still in passive state. This type of substitution in coated samples could be a viable source for improving the corrosion resistance of surgical grade 316 L SS for enhancing the biocompatibility of implant devices.
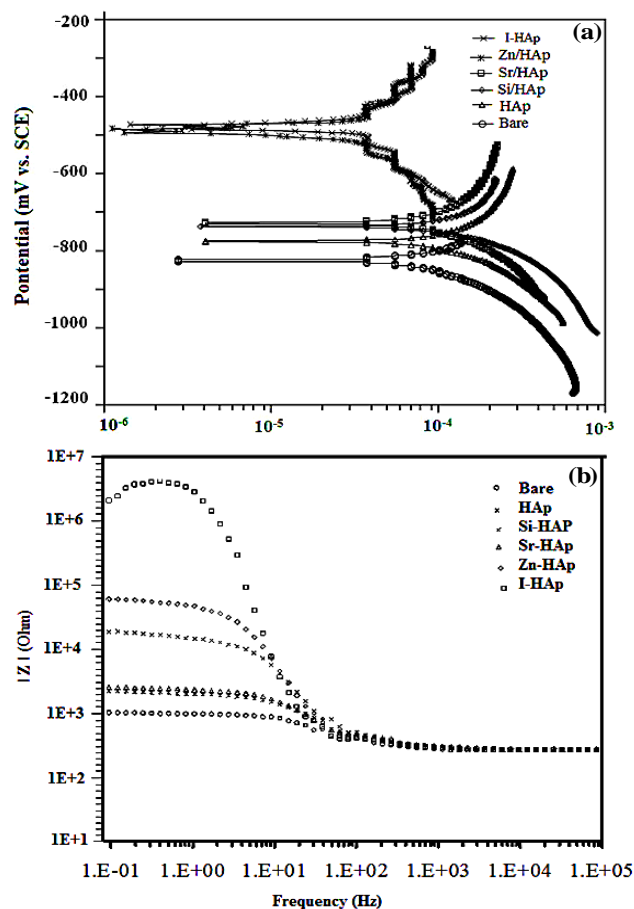

Fig. 6. Potentiodynamic (a) Polarisation curves and (b) Impedance spectra of Bare, HAp, Si-HAp, Sr-HA, Zn-HAp and I-Hap.

Table. 2. Polarization and Impedance analysis of bare, HAp, Si-HAp, Sr-HAp, Zn-HAp and I-HAp coated on 316L SS.

S.No	Samples	E corr (mV)	Icorr (μAcm^{-2})	Total impedance (|Z|)($\times 10^4$ Ω cm^2)	Polarisation Resistance (Rp)($\times 10^5$ Ω cm^2)	Capacitance (C) ($\times 10^{-5}$ Ω cm^2)
1	Bare	-821	1.12	7.54	3.9	3.8
2	HAp	-775	1.02	10.921	7.6	3.4
3	Si/HAp	-732	0.62	15.353	8.9	3.1
4	Sr/HAp	-728	0.30	17.849	11.8	2.5
5	Zn/HAp	-508	0.28	19.754	13.2	2.3
6	I-HAp	-422	0.25	21.78	15.69	1.9

Conclusion

In the present work pure and different ions substituted HAp were prepared by chemical precipitation method and sintered at 900 °C for 2 h. These samples were coated on surgical grade 316 L SS substrate using EPD technique and annealed at 400 °C for 2 h. The obtained coatings were homogeneous and showed a very good adhesion on the metal substrate. *In-vitro* biomineralization ability analysis with SBF solution confirmed that the apatite was completely covered the film in 21 days. The cyclic

polarization and corrosion potentials for all the HAp and I-HAp coated samples were found to be nobler than the pristine 316 L SS. The results of the coated samples demonstrated the improved corrosion resistance over the uncoated samples. The structural, morphological and electrochemical studies of HAp and I-HAp coatings on 316 L SS confirmed the possibility of these bioceramic coatings for bio implant applications.

Author contributions

Conceived the plan: K PA; Performed the experiments: K PA; Data analysis: K PA; Wrote the paper: K PA; Supervised the work: A MB, DM A JN, S PJ, THO; Authors have no competing financial interests.

Supporting informations

Supporting information is freely available from VBRI press.

Reference

1. González, Kaili, L.; Yanling, Z.; Yue, Z.; Haiyun, Q.; Feng, C.; Yingjie, Z.; Jiang, *C. Mater. Chem.,* **2011**, *21*, 16558.
   DOI: 10.1039/C1JM12514A
2. Gopi, D.; Nithiya, S.; Shiny joy, E.; Kavitha, *L. Spectro. Chim. Acta Part A.,* **2012**, *92*, 194.
   DOI: 10.1016/j.saa.2012.02.069
3. Boanini, E.; Gazzano, M.; *Bigi. A. Acta. Biomat*., **2010**, *6*, 1882.
   DOI: 10.1016/j.actbio.2009.12.041
4. Nasser, Y.; Hassan, M.; Omar, H.; *J. Am. Ceram. Soc*., **2011**, *94*, 1584.
   DOI: 10.1111/j.1551-2916.2010.04282.x
5. Kentaro, N.; Takashi, K.; Chiya, N.; Takamasa, O.; N. Atsushi. *Mater Trans.*, **2009**, *50*, 1046.
   DOI: 10.2320/matertrans.MC200808
6. Balamurugan, A.; Benhayoune, H.; Dumelie, N.; Laquerriere, P.; Ferreira. J. M. F.; *J. Am. Ceram. Soc.,* **2008**, *91*, 2797.
   DOI: 10.1111/j.1551-2916.2008.02513.x
7. Kannan, S.; Ventura, J. M.; Ferreira, J. M. F.; *Chem. Mater*., **2005**, **17**, 3065.
   DOI: 10.1021/cm050342+
8. Kannan, S.; Lemos, I. A. F.; Rocha, J. H. G.; Ferreira, J. M. F. J.; *Solid State. Chem.*, **2005**, *178*, 3190 .
   DOI: 10.1016/j.jssc.2005.08.003
9. Kannan, S.; Vieira, S.I.; Olhero, S.M.; Torres, P.M.C.; Pina , S.; da Cruz e Silva, O.A.B.; Ferreira, J.M.F.; *Acta. Biomater.*, **2011**, *7*, 1835.
   DOI: 10.1016/j.actbio.2010.12.009
10. Balamurugan, A.; Balossier, G.; Kannan, S.; Michel, J.; Faure, J.; Rajeswari, *S. Cera. Inter.,* **2007**, *33*, 605.
    DOI: 10.1016/j.ceramint.2005.11.011
11. Pietak, A.M.; Reid, J.W.; Stott, M.J.; Sayer, *M. Biomaterials.*, **2007**, *28*, 4023.
    DOI: 10.1016/j.biomaterials.2007.05.003
12. Gasqueres, G.; Bonhomme, C.; Maquet, J.; Babonneau, F.; Hayakawa, S.; Kanaya, T.; *Magn. Reson. Chem.*, **2008**, *46*, 342.
    DOI: 10.1002/mrc.2109
13. Miyajin, F.; Kono, Y.; Suyama, Y.; *Mater. Res. Bull*., **2005**, *40*, 209.
    DOI: 10.1016/j.materresbull.2004.10.020
14. Reginster, J.Y.; Bruyere, O.; Sawicki, A.; Roces-Varela, A.; Fardellone, P.; Roberts, A., et al. *Bone.*, **2009**, *45*, 1059.
    DOI: 10.1016/j.bone.2009.08.004
15. Li, Z.Y.; Lam, W.M.; Yang, W.M, C.; Xu, B.; Ni, G.X.l Abbah, S.A.; et al. *Biomaterial*., **2007**, *28*, 1452.
    DOI: 10.1016/j.biomaterials.2006.11.001
16. Ren, F.; Xin,R.; GE,X.; Leng, Y.; *Acta. Biomater.*, **2009**, *5*, 3141.
    DOI: 10.1016/j.actbio.2009.04.014
17. Tang. Y.; Chappell, H.F.; Dove, M.T.; Reeder, R.J.; Lee. Y.J.; *Biomaterial.,* **2009**, *30*, 2864.
    DOI: 10.1016/j.biomaterials.2009.01.043
18. Thian, ES.; Huang, J.; Best, SM.; et al. *Biomaterials.* **2005**; *26*, 2947.
    DOI: 10.1016/j.biomaterials.2004.07.058
19. Prem Ananth, K.; Suganya, S.; Mangalaraj, D.; Ferreira, J.M.F.; Balamurugan, A.; *Mater. Sci. and Engg. C.,* **2013**, *33*, 4160.
    DOI: 10.1016/j.msec.2013.06.010
20. Van der Biest, O.; Joos, E.; Vleugels, J.; Baufeld, *B. J Mater Sci.,* **2006**, *41*, 8086.
    DOI: 10.1007/s10853-006-0635-1
21. Balamurugan, A.; Balossier, G.; Michel, J.; Ferreira. J.M.F. *Electrochim Acta*, **2009**, *54*, 1192.
    DOI: 10.1016/j.electacta.2008.08.055
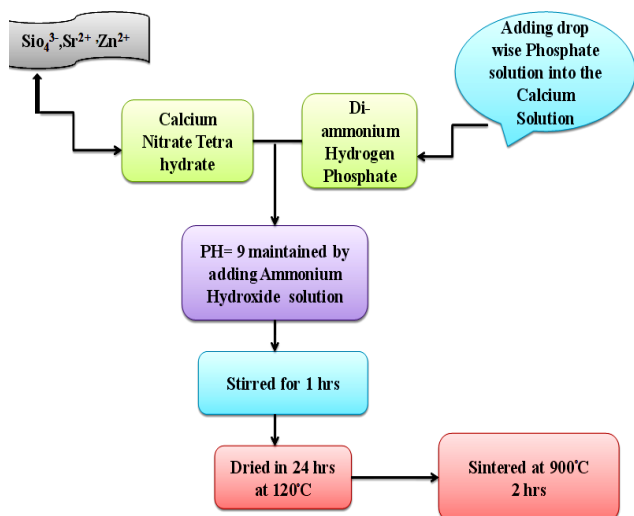
Supporting information

Fig. S1. Schematic diagram of the synthesis of pure HAp and I- HAp through chemical precipitation process.

Table S2. Reagents used for preparing SBF solution.

Order	Reagent	Amount(g/L)
1	NaCl	7.996
2	$NaHCO_3$	0.350
3	KCL	0.224
4	$K_2HPO_4.3H_2O$	0.228
5	$MgCl_2.6H_2O$	0.305
6	1M- HCL	40ml
7	$CaCl_2$	0.278
8	Na_2SO_4	0.071
9	$(CH_2OH)_3CNH_2$	6.057

Table S3. Quantitative EDX analysis for HAp, Si-HAp, Sr-HAp, Zn-HAp and I-HAp in Wt %.

Sample Name	Ca	P	Si	Sr	Zn	Ca/P	Ca+Sr+Zn /P+Si
HAp	34.50	15.91	-	-	-	1.67	1.67
Si-HAp	34.67	15.39	0.70	-	-	1.74	1.66
Sr-HAp	33.95	16.06	-	1.25	-	1.64	1.67
Zn-HAp	34.15	15.95	-	-	0.79	1.63	1.69
Si, Sr, Zn-HAp	35.20	15.28	0.68	1.37	0.85	1.77	1.72